

Lawrence Berkeley National Laboratory

Recent Work

Title

ELECTRICAL AND ELECTRON MICROSCOPY OBSERVATIONS ON DEFECTS IN ION IMPLANTED SILICON

Permalink

<https://escholarship.org/uc/item/9xm511hz>

Author

Ling, H.

Publication Date

1978-02-01

LBL-7386

C.2

ELECTRICAL AND ELECTRON MICROSCOPY OBSERVATIONS ON
DEFECTS IN ION IMPLANTED SILICON

H. Ling
(M. S. thesis)

February 28, 1978

RECEIVED
LAWRENCE
BERKELEY LABORATORY

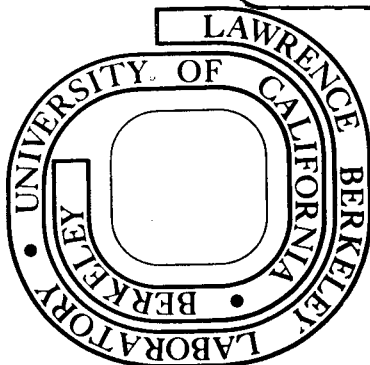
JUN 6 1978

LIBRARY AND
DOCUMENTS SECTION

Prepared for the U. S. Department of Energy
under Contract W-7405-ENG-48

TWO-WEEK LOAN COPY

*This is a Library Circulating Copy
which may be borrowed for two weeks.
For a personal retention copy, call
Tech. Info. Division, Ext. 6782*



LBL-7386

C.2

DISCLAIMER

This document was prepared as an account of work sponsored by the United States Government. While this document is believed to contain correct information, neither the United States Government nor any agency thereof, nor the Regents of the University of California, nor any of their employees, makes any warranty, express or implied, or assumes any legal responsibility for the accuracy, completeness, or usefulness of any information, apparatus, product, or process disclosed, or represents that its use would not infringe privately owned rights. Reference herein to any specific commercial product, process, or service by its trade name, trademark, manufacturer, or otherwise, does not necessarily constitute or imply its endorsement, recommendation, or favoring by the United States Government or any agency thereof, or the Regents of the University of California. The views and opinions of authors expressed herein do not necessarily state or reflect those of the United States Government or any agency thereof or the Regents of the University of California.

ELECTRICAL AND ELECTRON MICROSCOPY OBSERVATIONS
ON DEFECTS IN ION IMPLANTED SILICON

H. Ling

(M. S. Thesis)

February 28, 1978

Contents

Abstract 1

Introduction 3

Experiments I 6

Results and Discussion 7

 A. Electrical Properties 7

 B. Electron Microscopy Observation of Damage Structure . . 9

Conclusions 12

References 13

Acknowledgement 16

Figure Captions 17

Figures 19

ELECTRICAL AND ELECTRON MICROSCOPY OBSERVATIONS
ON DEFECTS IN ION IMPLANTED SILICON

H. Ling

Materials and Molecular Research Division
Lawrence Berkeley Laboratory
University of California
Berkeley, California

ABSTRACT

Silicon single crystals were implanted with 100 KeV phosphorous ions to a dose of 2×10^{16} ions/cm² at both room-temperature and 600°C. They were isochronally annealed at temperatures ranging from 400°C to 900°C. Sheet resistivity measurements of the specimens were taken after each anneal, together with corresponding transmission electron micrographs.

The observations show that when a completely amorphous layer is produced by ion implantation at room-temperature, epitaxial recrystallization onto the single crystal substrate during annealing at 600°C leaves a dislocated surface containing secondary defects. There appear to be a significant difference in the number of defects per implanted ion between room-temperature and 600°C implants, when annealing to 800°C and 900°C.

Sheet-resistivity measurement showed that, above a critical dose, room temperature implantation followed by a 600°C post anneal is substantially more effective for achieving electrical activity of the phosphorous than is implantation at 600°C. But 600°C implantation followed by 800°C and 900°C post annealed is more effective than room-temperature implantation.

The observed annealing behavior is explained in terms of defects that form during the recrystallization process.

INTRODUCTION

For heavy ions of phosphorous implanted into silicon at room-temperature zones of severely damaged material are produced in addition to isolated point defects around the periphery of the zones. If the damage is not annealed during the implantation, an amorphous layer is eventually formed where the individual damage zones overlap. (1.2)

An annealing treatment is then required both to return the sample to crystallinity and to put the phosphorous atoms onto electrically active sites (generally assumed to be substitutional positions).

It is thought that the activation energy for epitaxial recrystallization depends on the Radius of the amorphous region and to a very rough approximation, the ratio of the recrystallization temperature for an amorphous region of radius R to that for an infinite volume (e.g. a flat interface) is given by

$$\frac{T_r}{T_\infty} = 1 - \frac{2\gamma_i w}{RE_\infty}$$

where γ_i is the interfacial free energy between crystalline and amorphous Si, w is the activation volume for recrystallization (i.e. the volume of the 5 atom agglomerations which constitute amorphous Si, and E_∞ is the activation energy for an infinite interface. Choosing reasonable values for $\gamma_i = 500 \text{ erg cm}^{-2}$, $w = 2 \times 10^{-22} \text{ cm}^{-3}$ and $E_\infty = 5 \text{ ev}$, the annealing temperature curve as a function of zone size can be determined. The temperature is about 600°C where zones of $\sim 200\text{\AA}$ have to be recrystallized. One can avoid the formation of an amorphous layer by holding the substrate at higher temperature during implantation. (1.2)

For implantation performed at 600°C , a disordered region anneals

individually before the next ion strikes in its vicinity, thus preventing formation of the continuous amorphous layer even for high dose implants.

The characteristics of implanted phosphorous ions in silicon have been investigated by several authors using either radio-tracer⁽³⁻⁴⁾ or electrical measurements.⁽⁵⁻¹³⁾ Also, secondary defects in ion-implantation silicon have been observed by transmission electron microscopy. However, correlations between such defects and electrical properties of the ion-implanted layers are incomplete. Sheet resistivity and electron microscope observations have been made for B⁺ implanted and annealed silicon by Bicknell and Allen. However, Bicknell et al. just investigated moderate doses which did not form continuous amorphous layers. Also, their characterization of the loops formed on annealing do not agree with similar observations in this laboratory.

In an effort to determine the effects of recrystallization according to these two different mechanisms on the secondary ion implantation defects, implants were performed to the same dose but at two different temperatures, room-temperature and 600⁰C. Transmission electron microscopy was used to study the detailed nature of secondary defects formed by the ion implantation and subsequent annealing. Four-point probe sheet-resistivity measurements^(23, 24) were used to study the electrical property changes during the annealing. The annealing characteristics of layers implanted into silicon at 100 KeV with dose 2×10^{16} ions/cm² were measured and observed following isochronal annealing to 900⁰C. Room-temperature implants remain amorphous below 600⁰C and are not useful for most practical applications. 900⁰C was chosen as the upper annealing limit beyond which long-range diffusion would destroy any

advantage of profile control offered by the ion implantation technique.

This thesis reports on the measurements and conclusions of the study to date.

EXPERIMENTAL

N-type silicon wafers, 5 Ω -cm of (111) and (100) orientations were irradiated at both room-temperature and 600°C, with phosphorous ions at 100 KeV to a dose of 2×10^{16} ions/cm². The dose was chosen so as to produce a continuous amorphous layer in the room-temperature implant.

Pieces 1/2 in. x 1/2 in. were scribed from both (100) and (111) wafers for sheet resistivity measurements. The sheet resistivity specimens were annealed isochronally from 600°C up to 900°C in 100°C intervals for 20 minutes in a quartz tube furnace with dry nitrogen passing through it. After annealing, the sheet-resistivity measurements were performed by the four-point probe technique. After measurement, the pieces were ultrasonically cut into discs of 3 mm in diameter. They were then chemically thinned in a solution made up of two parts (3HNO₃:1HF) to one part (2.5 gm I₂ in 1100 ml CH₃COOH). The thinned samples were examined in transmission in a JEM 7A and a Philips 301 transmission electron microscope operating at 100 KeV.

RESULTS AND DISCUSSION

A. Electrical Properties:

(I) Implantation at Room-Temperature:

The changes in resistivity of (111) and (100) specimens phosphorous implanted at 100 KeV at room-temperature are shown in Fig. 1 during an isochronal annealing sequence.

There is a steady decrease in sheet resistance, between room-temperature to 600°C, as the anneal temperature increases. Webber, Thorn and Large⁽²²⁾ have shown that carrier mobility remains approximately constant in this region whilst the number of carriers increases. The steep fall in sheet resistance between 300°C and 600°C is due to annealing out of primary damage as the amorphous layer recrystallizes epitaxially onto the single crystal substrate. As indicated in the figure, approximately 80 percent of the implanted phosphorous atoms were on active sites following a 600°C anneal. The remaining 20 percent did not become active until annealing to a temperature of 900°C.

The sheet resistivity shows a steady decrease over the temperature region between 600°C and 900°C, but since the carrier mobility remains reasonably constant,⁽²²⁾ it is apparent that more carriers are becoming active. This also is confirmed by early work.⁽²³⁻²⁶⁾ The good agreement between the phosphorous concentration profile after annealing at 600°C and 800°C suggests that very little long-range diffusion takes place during isochronal annealing between

those two temperatures and that the observed fall in sheet resistance is simply due to an increase in the number of active carriers.

(II) Implantation at 600°C :

Implantation at 600°C and the consequent annealing out of each individual ion track as it is formed prevents any build up of primary damage and the formation of a continuous amorphous layer. In this case, the sheet resistance of the implanted layer was initially higher than that which would be achieved in a room-temperature implanted specimen after 600°C unannealing. The sheet resistivity then fell continuously with increasing annealing temperature above 600°C . Comparison of these two implantation conditions by Shannon, Ford and Gard⁽¹³⁾ have shown that the profiles of electrically active phosphorous suggests that the implantations made at 600°C where damage was being continuously annealed out enabled more of the implanted ions to enter channels throughout the duration of the implant and thus form a more pronounced tail on the depth distribution. Calculation of the total number of carriers to be expected for these two profiles suggests that the concentration of active phosphorous in the 600°C implantation should be somewhat below that achieved for a room-temperature implanted specimen which has been annealed at 600°C . This can account in part for the higher sheet resistance measured following the 600°C anneal of a layer implanted at 600°C

as compared to a room-temperature implanted specimen.

From our results, complete electrical activity (Max. number of carriers) is not observed until annealing to nearly 800°C. This necessity for high annealing temperature to achieve substantially complete activity of the phosphorous is found in almost all cases⁽⁶⁾ where a continuous amorphous layer is not formed during implantation. This has been attributed to the presence of electrically active defect centers⁽¹⁷⁾ ⁽²⁵⁾ which compensate the dopant behavior of the implanted atoms.

B. Electron Microscope Observation of Damage Structure:

A series of micrographs and diffraction patterns obtained by transmission electron microscopy is shown in Figure 2-7.

(I) Implanted at Room Temperature:

A. At Unannealed State:

Figure 2 is a micrograph of the edge region of a specimen of silicon, having the (100) plane parallel to its surface. The region A, shows very strong amorphous diffraction rings; in region B, the selected area diffraction pattern consists of several diffuse rings as well as crystalline spots, and in region C, there is only a single crystal diffraction pattern. This confirms that a buried amorphous layer is sandwiched between a thin crystalline layer at the surface and the underlying crystal substrate.

Many small (100-200 Å) dark spots are seen in bright field micrograph (light spots in dark field). We believe

these spots are in the crystalline-amorphous interface since they are not found in specimens where the amorphous layer can be observed alone with the crystalline material stripped away. Also, these spots are strongly visible in dark field only when a crystalline reflection is selected rather than a diffuse ring arising from the amorphous material.

B. Annealed to 600°C-800°C:

At 600°C, recrystallization of the amorphous layer had occurred epitaxially so that the single crystal is reformed. The point defects develop into secondary defects which become visible by transmission electron microscopy such as black dot defects, perfect and faulted dislocation loops, dislocation dipoles. As seen from Figure 4 and 6 with increasing of annealing temperatures, dislocation loop density decreases and the average diameter of loops increases. These loops were analyzed by tilting the specimen in the microscope and examining both dark and bright field images. All these dislocation loops were determined to be interstitial type. (27,28,29,30) The streaking in the diffraction pattern could arise from thin platelets or rods and could be caused by a high concentration of dislocation loops lying on planes perpendicular to the foil surface.

C. Annealed to 900°C:

Dislocation networks were generated lying approximately parallel to the foil surface. It was confirmed by Tamura⁽³⁰⁾ using the $g \cdot b = 0$ criterion that the dislocation segments

comprising the network were all pure edge type lying approximately along the 211 directions. Burgers vectors were of the $\frac{a}{2}\langle 110 \rangle$ type in the (111) film plane.

(II) Implanted at 600°C:

A. Figure 5 shows that an amorphous layer was no longer formed during implantation; black dot defects and complex dislocation entanglements were observed.

B. Annealed to 800°C:

Figure 6A and 6B shows these defects grew into dislocation loops. Comparing these pictures 6A, 6B, 6C and 6D shows that defect density is different. It can be seen that 600°C implantation followed by an 800°C post anneal 20 minutes results in lower defect density. This may explain why we get lower resistivity in 600°C implantation followed by an 800°C post annealing.

CONCLUSION

A detailed examination of the changes in electrical conductivity and secondary defects formed during post implantation annealing of phosphorous-implanted silicon has led to the following observations and conclusions:

- (i) The results presented show a strong correlation between the electrical activity of phosphorous implanted silicon and its appearance in the electron microscope (e.g. the kind of defects, density of defects).
- (ii) It can be seen that 600^oC implantation followed by 800^oC annealing reduces the defect density compared to room-temperature implantation and 800^oC annealing.
- (iii) For every room-temperature implantation report to date in which a large increase in number of carriers was found near 600^oC annealing temperature, the total ion dose was sufficiently high to have formed an amorphous layer. If an amorphous layer is not formed (hot-substrate implantations), annealing temperatures of at least 700-750^oC are required for the number of carriers to reach its maximum value.

REFERENCES

1. D. J. Mazey, R. S. Nelson, and R. S. Barnes, *Phil. Mag.* 17 1145 (1968).
2. B. L. Crowder, R. S. Title, *Rad. eff.* 6, 63 (1970).
3. G. Dearnaley, J. H. Freeman, G. A. Gard, and M. A. Wilkins, *Canad. J. Phys.*, 46, 587 (1968).
4. J. F. Gibbons, A. El-Hoshy, K. F. Manchester, and F. L. Vogel, *Appl. Phys. Letters*, 8, 46 (1966).
5. V. M. Gusev, M. I. Guseva, V. I. Kurinny, V. G. Naumenko, V. V. Titov, and V. S. Tsyplenkov, *Proc. Inter. Conf. on Radiation Effects in Semiconductors*, Toulouse (1967).
6. V. K. Vasil'ev, E. I. Zorin, P. V. Pavlov, and D. Tetel'baum, *Fizika Tverdogo Tela*, 9, 1905 (1967).
7. W. M. Gibson, F. W. Martin, R. Steusgaard, F. P. Jensen, N. I. Meyer, and G. Galster, *Canad. J. Phys.*, 46, 675 (1968).
8. D. E. Davies, *Appl. Phys. Letters*, 14, 227 (1969).
9. B. L. Growder and F. F. Morehead, Jr., *Appl. Phys. Letters*, 14, 331 (1969).
10. J. H. Freeman, *Proc. Int.-Com. Appl. for Beams to Semiconductor Technology*, Grenoble, France (1967), p. 75.
11. R. L. Petritz, *Phys. Rev.*, 110, 1254, (1958).
12. G. Dearnaley, M. A. Wilkins, P. D. Goode, J. H. Freeman, and G. A. Gard, A. E. R. F. R6197 (1969 (To be published in the *Proceeding of the Sussex Conference on Atomic Collision Phenomena in Solids*, Sept., 1969)).

13. J. M. Shannon, R. A. Ford, C. A. Gard "Ion Implantation", Gordon and Breach, Science Publishers (1970).
14. L. N. Large, R. W. Bicknell, J. Materials Sci., 2, 589 (1967).
15. M. D. Matthews, R. F. James, Phil. Mag., 13, 1179 (1969).
16. S. M. Irving, Proc. Internat. Conf. Si Science and Technol., New York (1969).
17. R. W. Bicknell, R. M. Allen, Proc. Internat. Conf. Ion Implementation in Semiconductors, Thousand Oaks, (1970).
18. L. T. Chadderton, F. H. Eisen, *ibid.*
19. S. M. Davidson, G. R. Booker, *ibid.*
20. S. M. Davidson, Proc. European Conf. on Ion Implantation, Reading, England, (1970).
21. M. Tamura, T. Ikeda, N. Yoshihiro, Proc. of the 2nd Conf. on Solid State Devices, Tokyo, Japan (1970).
22. R. F. Webber, R. S. Thorn, and L. N. Large, Int. J. Electronics, 26, 163 (1969).
23. E. Tennenbaum, Solid State Electronics, 2, 123 (1961).
24. J. C. Irvin, Bell System Tech. J., 41, 387 (1962).
25. J. W. Meyer, O. J. Marsh, G. A. Shifrin, and R. Baron, Canad. J. Phys, 45, 4073 (1967).
26. E. H. Putley, The Hall Effect and Related Phenomena, Butterworths, London (1960).
27. K. Seshan and J. Washburn, 1974, Phys. Stat. Sol. (a), 26, 345.
28. K. Seshan and J. Washburn, 1975, Radiat. Effects, 26, 31.

29. M. Tamura, T. Ikeda, and W. Yoshihiro, 1971, Proceedings of the 2nd Conference on Solid State Devices, Tokyo, p. 9.
30. M. Tamura, 1977, Phil. Mag. 35, 663.

FIGURE CAPTIONS

- Fig. 1. (a) The sheet resistance of phosphorous layers implanted into silicon at both room temperature and 600°C. Measurements are made following each successive isochronal annealing.
- Fig. 2. (a) A bright field image of a N-type (100) silicon sample irradiated with 2×10^{16} p ions/cm² at room temperature. A buried amorphous layer is sandwiched between a thin crystalline layer at the surface and the underlying crystal substrate. The region marked A shows very strong amorphous diffraction rings and region B shows a crystalline-amorphous interface. The region C is a thick region which just shows a crystalline pattern.
- (b) Shows a dark field image by placing the objective aperture at the crystal spot. Light spots are believed to be islands of crystal near the crystalline amorphous interface.
- Fig. 3 Shows bright field image and dark field image of a N-type (111) silicon sample irradiated with 2×10^{16} p ions/cm² at room temperature.
- Fig. 4 (a) A (111) orientation N-type silicon film bombarded with 2×10^{16} , 100 KeV p ions/cm² and annealed for 20 minutes at 600°C. Epitaxial recrystallization occurs.
- (b) (100) orientation.
- Fig. 5 (a) Shows a bright field image of (111) orientation N-type silicon film bombarded with 2×10^{16} p ions/cm² at 600°C.

An amorphous layer is no longer formed during the implantation. Black dot defects and complex dislocation entanglement were observed.

(b) (100) orientation.

Fig. 6 All specimens were implanted with 2×10^{16} p ions/cm² at 100 KeV and then annealed for 20 min. at 800°C.

(a) The (111) orientation implanted at 600°C.

(b) The (100) orientation implanted at 600°C.

(c) The (111) orientation implanted at room-temperature.

(d) The (100) orientation implanted at room-temperature.

Fig. 7 All specimens were implanted with 2×10^{16} pt/cm² at 100 KeV and then annealed for 20 min. at 900°C.

(a) The (111) orientation implanted at 600°C.

(b) The (100) orientation implanted at 600°C.

(c) The (100) orientation implanted at room-temperature.

(d) The (100) orientation implanted at 600°C.

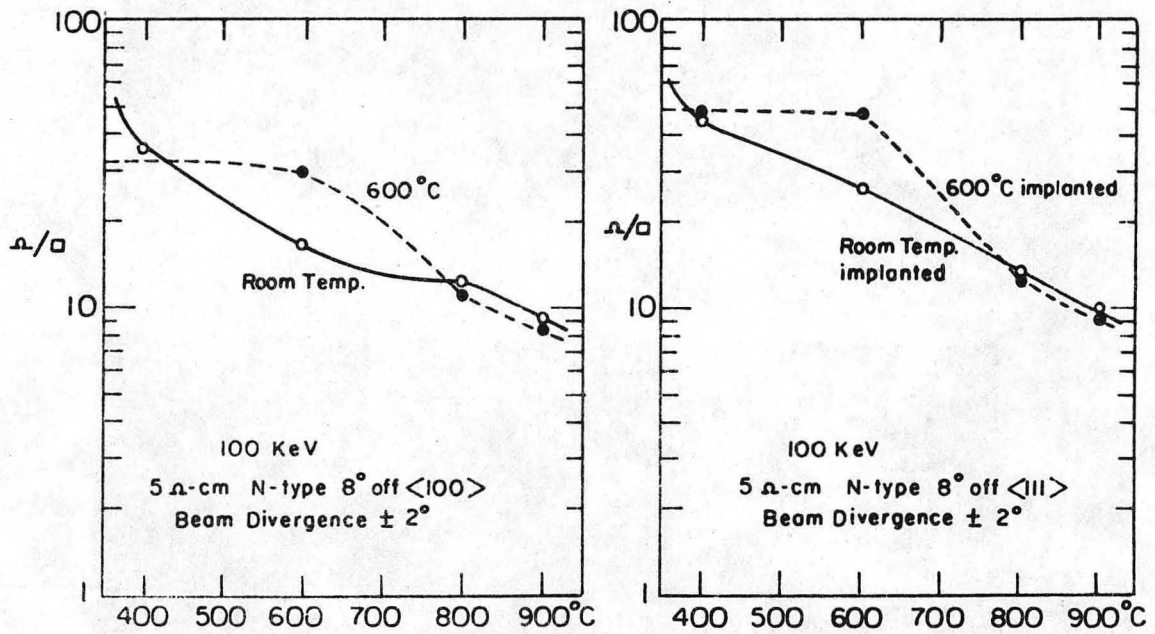
ACKNOWLEDGMENT

The author wishes to express his gratitude to Professor Jack Washburn for his guidance in this research. Many helpful discussions with other members of Washburn's group in the Materials Science Department at Berkeley are also acknowledged.

Love and encouragement from the author's family members such as his parents (Mr. and Mrs. C. S. Ling), his brothers and, of course, his wife, Chaoching, are highly appreciated. Without their help, it would have been impossible for the author to be able to study here in Berkeley.

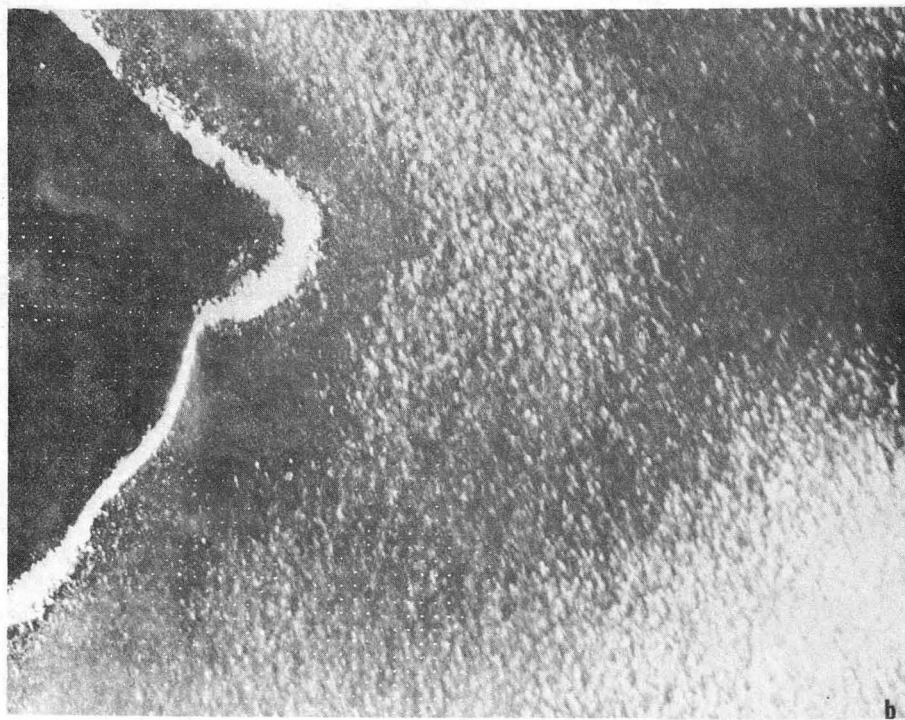
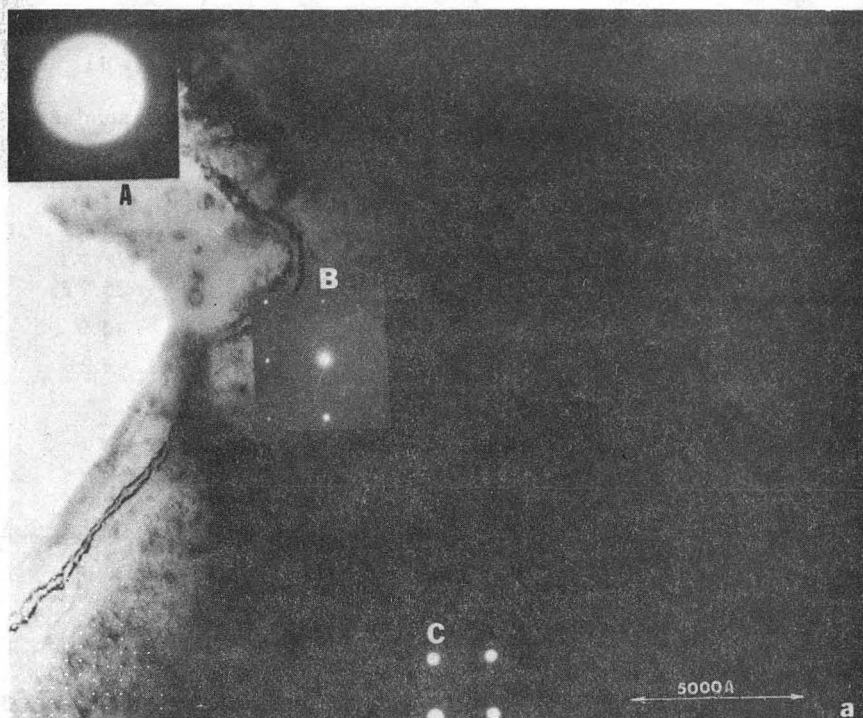
This work was supported by the U.S. Energy Research and Development Administration through the Materials and Molecular Research Division of the Lawrence Berkeley Laboratory, Berkeley, California.

(100)			(111)		
Annealing Temperature °C	Implanted at Room Temp. Ω/\square	Implanted at 600°C Ω/\square	Annealing Temperature °C	Implanted at Room Temp. Ω/\square	Implanted at 600°C Ω/\square
Room Temp.	115.7	35.56	Room Temp.	156.42	53.34
400	37.4	32.96	400	43.28	47.87
600	16.33	29.9	600	25.72	46.68
800	12.66	11.97	800	13.9	13.42
900	9.09	8.63	900	9.96	9.10



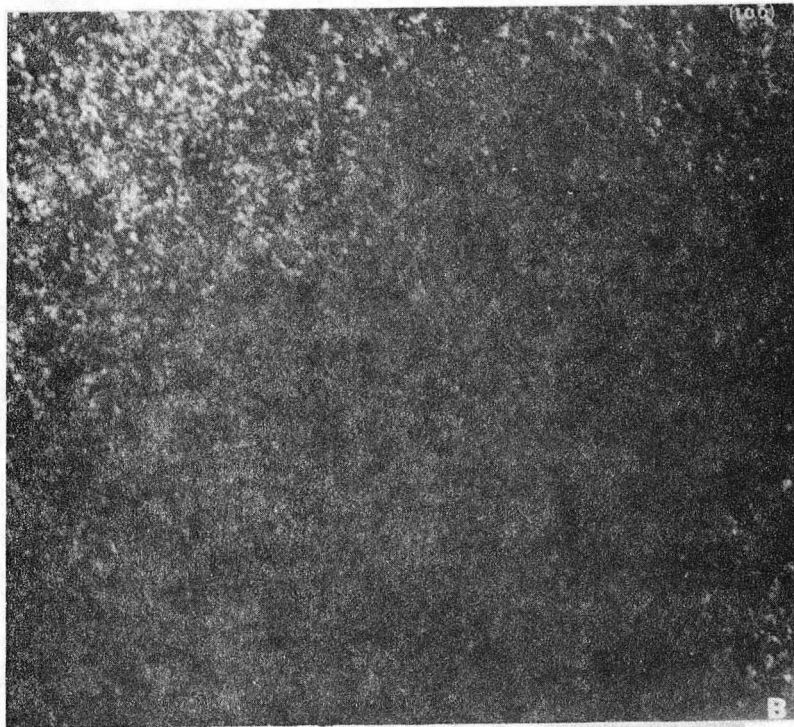
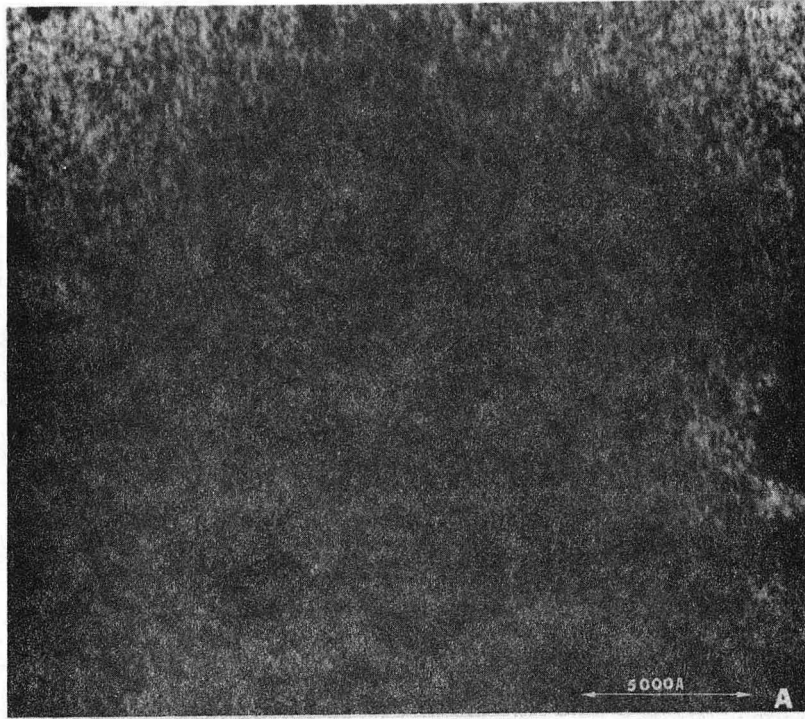
XBL 782 - 4 555

Fig. 1



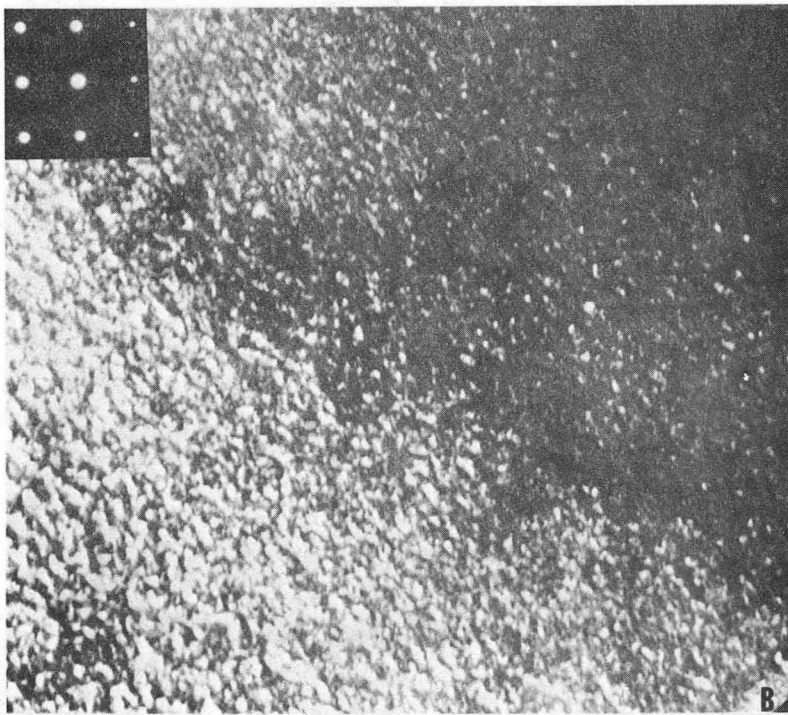
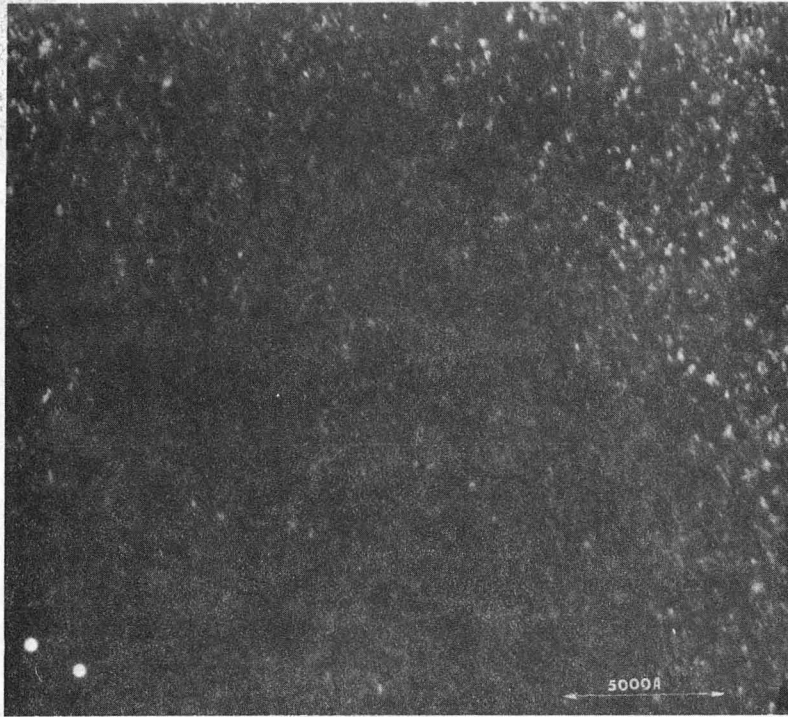
XBB 782-2174

Fig. 2



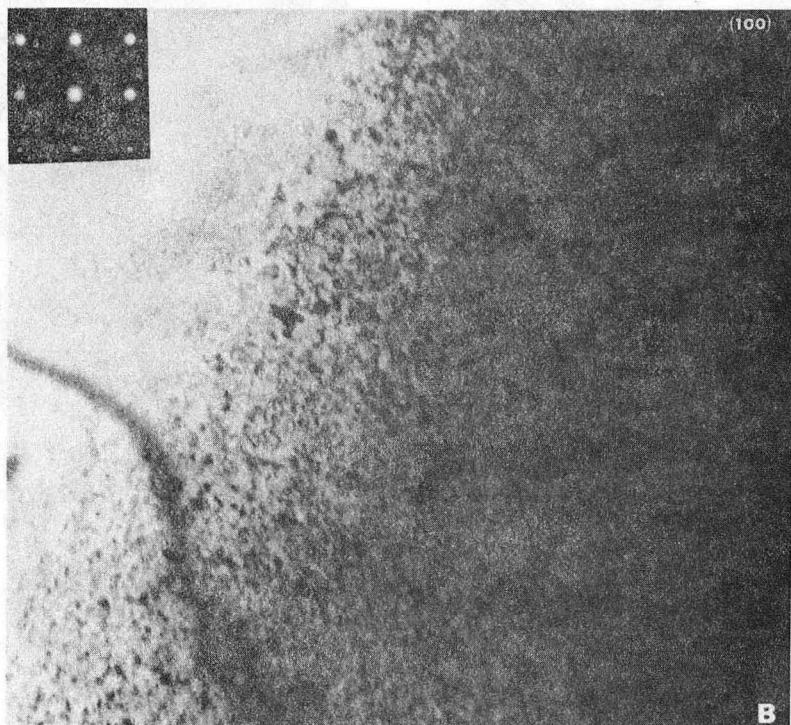
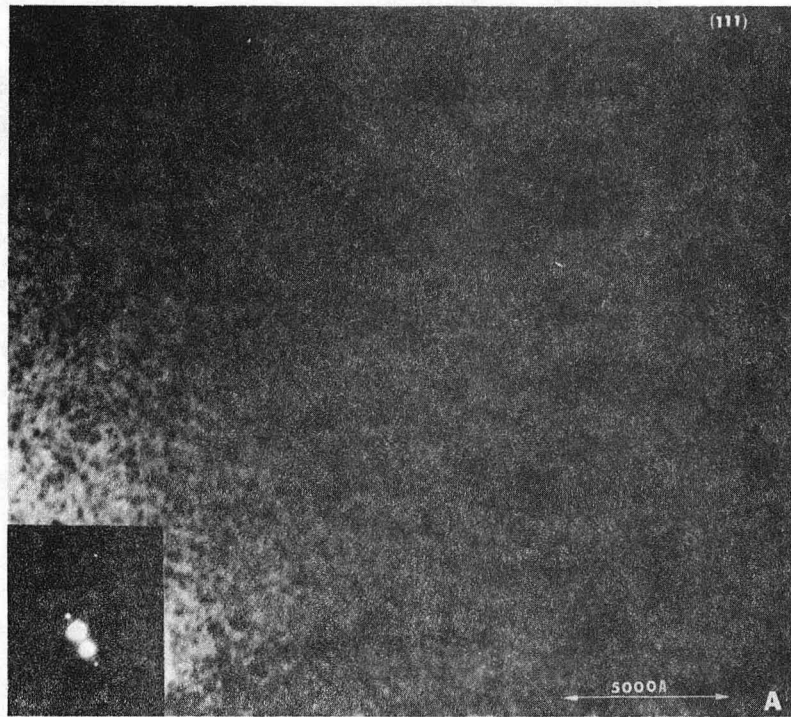
XBB 782-2175

Fig. 3



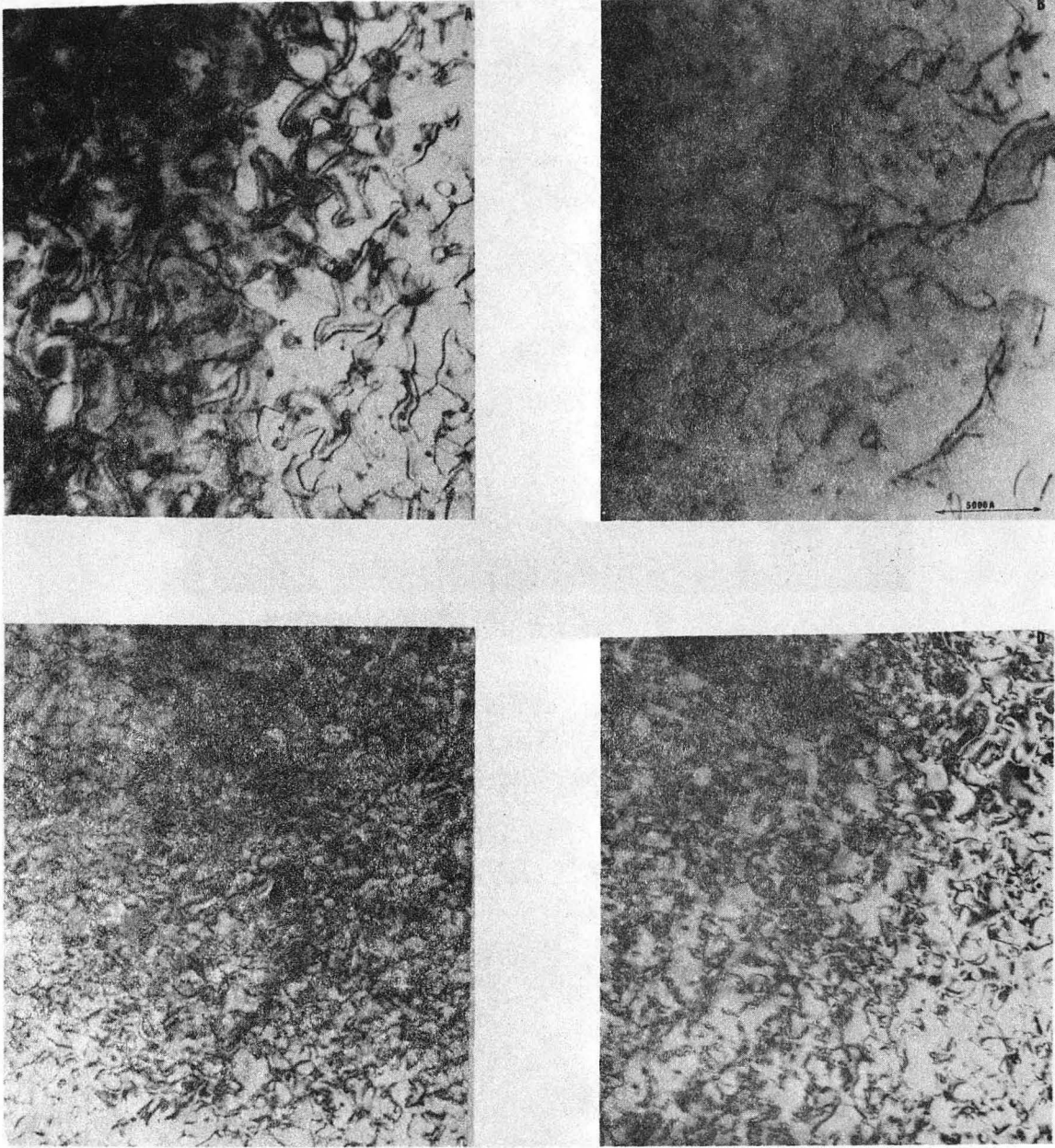
XBB 782-2171

Fig. 4



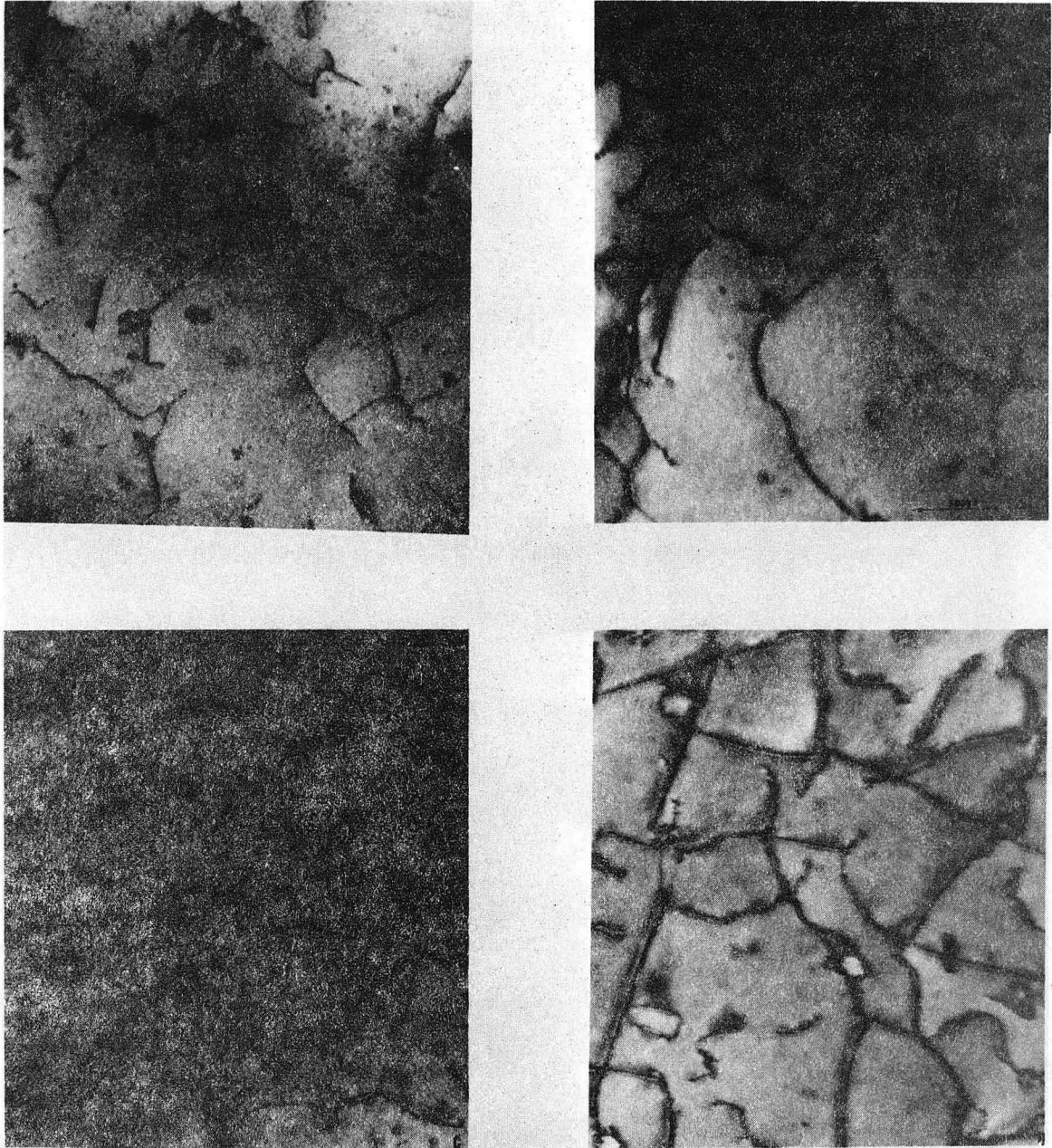
XBB 782-2170

Fig. 5



XBB 782-2173

Fig. 6



XBB 782-2172

Fig. 7

This report was done with support from the Department of Energy. Any conclusions or opinions expressed in this report represent solely those of the author(s) and not necessarily those of The Regents of the University of California, the Lawrence Berkeley Laboratory or the Department of Energy.

TECHNICAL INFORMATION DEPARTMENT
LAWRENCE BERKELEY LABORATORY
UNIVERSITY OF CALIFORNIA
BERKELEY, CALIFORNIA 94720